A low molecular weight alginate oligosaccharide disrupts pseudomonal microcolony formation and enhances antibiotic effectiveness

Manon F. Pritchard,[a#] Lydia C. Powell,[a] Alison A. Jack,[a] Kate Powell,[a] Konrad Beck,[a] Hannah Florance,[b] Julian Forton,[c] Philip D. Rye,[d] Arne Dessen,[d] Katja E. Hill,[a] David W. Thomas[a]

Advanced Therapies Group, Cardiff University School of Dentistry, Cardiff, UK[a]; Department of Biosciences, College of Life and Environmental Sciences, Exeter University, Exeter, UK[b]; Childrens Hospital of Wales, Paediatric Respiratory Medicine, Cardiff, UK[c]; AlgiPharma AS, Sandvika, Norway[d]

Running Head: OligoG CF-5/20 disrupts pseudomonal microcolonies

#Address correspondence to Manon Pritchard, pritchardmf@cardiff.ac.uk.

Present address:

- Alison A. Jack, Cultech Limited, Port Talbot, UK.
- Hannah Florance, UK Centre for Mammalian Synthetic Biology, The King's Buildings, Edinburgh, UK.

ABSTRACT

In chronic respiratory disease the formation of dense, 3-dimensional 'micro colonies' by *Pseudomonas aeruginosa* within the airway plays an important role in contributing to resistance to treatment. An *in vitro* biofilm model of pseudomonal microcolony formation using artificial sputum (AS) medium was established to study the effects of low molecular weight alginate oligomers (OligoG CF-5/20) on pseudomonal growth, microcolony formation and the efficacy of colistin. The studies employed clinical cystic fibrosis (CF) isolates (n=3) and reference non-mucoid and mucoid multi-drug resistant (MDR) CF isolates (n=7). Bacterial growth, biofilm development and disruption were studied using cell-viability assays and image analysis using scanning electron- and confocal laser scanning microscopy. Pseudomonal growth in AS medium was associated with increased ATP production ($p<0.05$) and the formation (at 48 h) of discrete (>10 μm) microcolonies. In conventional growth medium, colistin retained an ability to inhibit growth of planktonic bacteria, although the MIC was increased (0.1 to 0.4 μg/ml) in AS medium versus. In contrast, in an established biofilm model in the AS medium, the efficacy of colistin was decreased. OligoG CF-5/20 ($\geq$2%) treatment however, induced dose-dependent biofilm disruption ($p<0.05$), and led to colistin retaining its antimicrobial activity ($p<0.05$). Whilst circular dichroism indicated that OligoG CF-5/20 did not change the orientation of the alginate carboxyl groups, mass-spectrometry demonstrated that the oligomers induced dose-dependent (>0.2%; $p<0.05$) reductions in pseudomonal quorum sensing signaling. These findings reinforce the potential clinical significance of microcolony formation in the CF lung, and highlight a novel approach to treat MDR pseudomonal infections.

Keywords: *Pseudomonas aeruginosa*, colistin, cystic fibrosis, alginate, OligoG CF-5/20

The opportunistic Gram-negative pathogen *Pseudomonas aeruginosa* is found in a range of chronic human respiratory diseases, including chronic obstructive pulmonary disease and cystic fibrosis (CF) (1). CF is a life-threatening, autosomal recessive genetic disorder affecting 1 in 2,300 Caucasian live births (2). Reduced airway surface-liquid volume and abnormally viscous sputum result in ineffective mucociliary clearance (3). Chronic bacterial colonization of the lung by a number of opportunist pathogens occurs, most notably *P. aeruginosa,* which will predominate with time (4).

Within the diseased lung, patho-adaptive mutation results in the selection of hypermutator *P. aeruginosa* strains (5, 6). In *P. aeruginosa* this adaption occurs with a switch to the mucoid phenotype, characterized by over-production of high molecular weight (Mw; >15 kDa) alginate exopolysaccharide (EPS) (7, 8). This switch is accompanied by modification of acyl homoserine lactone (AHL) and *Pseudomonas* quinolone signal (PQS)-dependent quorum sensing (QS) systems (9), with altered production of virulence factors e.g. pyocyanin and hydrogen cyanide (10). Extracellular alginate affords protection from host innate immune-responses, including phagocytosis and neutrophil-derived reactive oxygen species (11). Mucoidal pseudomonal strains are often un-responsive to aggressive antibiotic selection (12) and 18.1% of CF patients are colonized with multi-drug resistant (MDR) *P. aeruginosa* (13).

In contrast to standard laboratory models of bacterial biofilm formation on material surfaces, biofilms within the CF lung form as non-adherent spherical microcolonies, embedded in respiratory mucin (14, 15). Whilst *in vitro* studies of *P. aeruginosa* from CF lungs routinely employ nutrient-rich media to optimize bacterial growth, or Mueller-Hinton (MH) medium, such media fail to adequately reproduce the lung environment or secretome (3). More recently, defined media such as artificial sputum (AS) medium (containing components of CF sputum e.g. DNA, mucin, mineral salts, proteins and amino acids) have been employed to model the behavior of *P. aeruginosa* (16-18). These AS medium models have been used to study the adaptation of pathogens to the CF lung using whole-genome

77 sequencing and microarray expression profiling (19), analyze diffusion (20) and test the
78 effectiveness of antibacterial therapeutics (21).

79 This distinctive biofilm microcolony formation in the CF lung has been demonstrated *ex-*
80 *vivo* in freshly-excised intraluminal material and in lung sections (14). Studies have also
81 further shown that *in vitro* biofilms observed in nutrient-limited conditions are increasingly
82 recalcitrant to antibiotic therapy due to enhanced tolerance (22). The design and delivery of
83 antimicrobial therapy targeted against the polymicrobial respiratory biofilm is, therefore,
84 challenging (23).

85 The acquisition of MDR *Pseudomonas* in the CF lung has led to a resurgence of clinical
86 interest in the bacteriocidal antibiotic colistin (24). Overlooked for many years due to
87 associated nephro- and neuro-toxicity (25, 26), colistin is increasingly used to treat life-
88 threatening infections (24) and as an inhaled therapy in CF to prevent establishment of
89 infection by MDR bacteria (25). While resistance to colistin remains low (27), the emergence
90 of colistin-resistant strains heralds fears of a post-antibiotic era (28).

91 We previously described the use of a low molecular weight alginate oligomer (OligoG
92 CF-5/20, ≥ 85% guluronic acid, with a degree of polymerization [DPn] of 16; Mn 3,200) from
93 the seaweed *Laminaria hyperborea* as a promising novel therapy in CF (29-31). *In vitro*
94 studies, demonstrated the ability of OligoG CF-5/20 to modify bacterial surface charge (30)
95 and biofilm growth of non-mucoid *Pseudomonas* sp. in conventional culture/biofilm models
96 (29). It is however, important to determine whether OligoG CF-5/20 could modify bacterial
97 growth within the inherently antibiotic-resistant microcolonies, which characterize the
98 diseased CF lung.

99 The objective of this study was to investigate the therapeutic efficacy of OligoG CF-5/20
100 and colistin in an *in vitro* microcolony model. We characterized the growth of fresh clinical
101 isolates from CF patients and strains from the International *P. aeruginosa* Reference Panel
102 (IPARP). Planktonic and biofilm cultures of wild-type PAO1 and the mucoid MDR
103 NH57388A were studied in MH and AS media. We developed microcolonies in the AS
104 medium and investigated the ability of OligoG CF-5/20 to modify these biofilms and further

105 determined the effectiveness of a combination treatment with colistin. The effect of colistin
106 on the mucoid CF isolate NH57388A grown under planktonic and biofilm conditions was
107 reduced in this AS medium. In contrast, OligoG CF-5/20 retained its dose-dependent anti-
108 biofilm properties, as well as maintaining the effectiveness of colistin *in vitro*, demonstrating
109 that addition of alginate oligosaccharides modifies pseudomonal microcolony assembly.
110

RESULTS

Non-mucoid *P. aeruginosa* IPARP have faster growth rates in MH medium than either mucoid or new non-mucoid CF isolates

Growth of non-mucoid *P. aeruginosa* in MH medium from the IPARP reference strains was more abundant (maximum absorbance ≥1) compared to the delayed, weaker growth of the fresh clinical isolates (maximum absorbance ≤1); acquiring stationary phase at 12 h versus 20 h respectively (**Fig. 1A**). The growth rates of the non-mucoid *P. aeruginosa* (PAO1, AA2, AA44) were also greater than those of the new CF Isolates (22476, 22078, 22554) and those of the mucoidal strains (AA43, IST27, 2192, NH57388A) from the IPARP collection (**Fig. 1B**) having doubling-times (at maximum exponential growth) of 0.2-0.23 versus 0.31-0.6 versus 0.29-0.56 unit/h respectively.

Colistin maintains its antimicrobial properties in the presence of the mucolytic OligoG CF-5/20

Initial studies on the effect of OligoG CF-5/20 and colistin (0.5x minimum inhibitory concentration [MIC] value) on pseudomonal growth in MH medium, demonstrated no difference in the growth rate of NH57388A when treated with colistin (0.16 unit/h) compared to the control (**Fig. 1C**), although a reduced growth rate (0.12 unit/h) was noted when treated with either 2% OligoG CF-5/20 or colistin with 2% OligoG CF-5/20. This was reflected by the significantly decreased cell biomass at stationary phase (36 h) following treatment with 2% OligoG CF-5/20 in combination with colistin compared to the control ($p<0.05$).

In the biofilm disruption assay, confocal laser scanning microscopy (CLSM) images of LIVE/DEAD®-stained, 24 h established pseudomonal biofilms demonstrated homogenous growth in the untreated control (**Fig. 1D**). Treatment for 1 h with colistin alone at 0.5x the minimum biofilm eradication concentration (MBEC value as previously described [32]) was associated with a decreased density of the resultant biofilm (**Fig. 1E**). Furthermore, when treated with 2% OligoG CF-5/20 alone for 1 h, the biofilm height was reduced and there was

increased porosity (**Fig. 1F**). Combination treatment of colistin and 2% OligoG CF-5/20 resulted in marked biofilm disruption (**Fig. 1G**). Quantification using COMSTAT image analysis software (33) revealed that biofilm height was significantly reduced from 11 ±4 μm (in the untreated control) to 1.1 ±0.2 μm following 2% OligoG CF-5/20 and colistin combination treatment (**Fig. 1H**). In parallel, the ratio of dead to live cells was significantly increased following treatment with colistin (0.24 ±0.07) or 2% OligoG CF-5/20 and colistin in combination (0.49 ±0.22) compared to the control (0.053 ±0.014; $p<0.05$; **Fig. 1I**); with associated increases in porosity.

Mucoid and non-mucoid *P. aeruginosa* show a distinctly altered biofilm phenotype in artificial sputum medium

Biofilms grown in different nutrient media exhibited distinct patterns of growth, with a marked phenotypic difference in biofilm architecture in MH- versus AS medium (**Fig. 2A-B;** diagrammatic representation **Fig. 2C**). Pseudomonal biofilms of both strains showed conventional homogenous growth in MH medium, whilst discrete, spherical microcolonies with an inter-linking network of extracellular polysaccharide (EPS) were apparent in AS medium. Microcolonies were not strongly bound to the well plates and varied considerably in size. The median diameter of the PAO1 and NH57388A microcolonies was 14 ± 4 μm and 11 ±5 μm respectively; the difference in size perhaps reflecting the slower growth rate of the mucoid strain. Elongated structures between the microcolonies were composed of linearly arranged bacterial cells.

Growth curves were performed using a cell-viability assay, (measuring ATP production); conventional growth curves with optical density measurements being impractical in AS medium, due to bacterial aggregation and microcolony formation. Marked differences in ATP production between cells grown in AS versus MH medium were evident within 24 h, being considerably elevated in AS medium (**Fig. 2D**).

OligoG CF-5/20 disrupts *P. aeruginosa* (NH57388A) microcolony formation in artificial sputum medium

SEM studies using a biofilm formation assay of *P. aeruginosa* (NH57388A) biofilms grown in MH medium ± OligoG CF-5/20 demonstrated the growth inhibitory effects of OligoG CF-5/20 at ≥2% (w/v; **Fig. 3A**), which was reflected in a corresponding reduction in EPS formation. Mucoid *P. aeruginosa* (NH57388A) formed typical microcolonies in AS medium at 48 h (**Fig. 3B**); with individual bacterial cells visible on the surface of the microcolonies encased in EPS (**Fig. 3C**). Biofilm formation in the presence of OligoG CF-5/20 was associated with a dose-dependent decrease in microcolony size and increasing cellular disruption of the biofilms. At 6% OligoG CF-5/20, the median microcolony diameter was 4.5 µm versus 6.6 µm in the untreated control (**Fig. 3D**). Corresponding CLSM images of Syto-9 and Concanavalin A 633 matrix-stained NH57388A 48 h biofilms in AS medium showed dense microcolonies surrounded by EPS (red) throughout the structure (**Fig. 3E**). Biofilms grown in OligoG CF-5/20 exhibited a decreased, overall biofilm mass with few spherical microcolonies and reduced EPS.

Using the biofilm disruption assay, CLSM images of matrix-stained NH57388A 48 h-established biofilms stained with Syto-9 (green) demonstrated large cellular aggregates or microcolonies (**Fig. 3F**) on (or within) a layer of cells. Treatment for 1 h with 2% OligoG CF-5/20, induced a reduction in aggregate size (**Fig. 3G**), with marked microcolony disruption. 3D videos of these images are available online (**Supplementary information Video 1**).

Circular dichroism spectra of OligoG CF-5/20 mixed with high molecular weight pseudomonal alginate do not indicate a specific interaction

Circular dichroism (CD) spectroscopy was used to test whether OligoG CF-5/20 and the high molecular weight EPS alginate produced by mucoid pseudomonal strains show a specific

interaction. The CD chromophore responsible for the Cotton effect observed at ca. 210 nm has been identified as the carboxyl groups of the alginates, and the n → π* transition reflects their orientation (34). Upon heating from 4 to 37°C, spectra of high Mw alginate showed no changes over a period of ~80 min (**Fig. 4A**, scans 1 to 7). Subsequent addition of OligoG CF-5/20 at a 50-fold molar excess resulted in an increased CD amplitude, i.e. more negative values (**Fig. 4A**, scans 8 to 11). Addition of Ca^{2+} to a final concentration of 1 mM had no effect (**Fig. 4A**, scans 12 to 17). The spectra observed for the high Mw alginate/OligoG CF-5/20 mixture corresponded to an additive effect of the two components not indicating any change in the orientation of the carboxyl groups (cf. dashed curves in **Fig. 4A**). Experiments in which Ca^{2+} was added to the high Mw alginate before the addition of OligoG CF-5/20, and a 1:600 molar ratio of high Mw alginate to OligoG CF-5/20 also are compatible with an additive effect with no indication of a change in the orientation of the carboxyl groups (**Fig. S1**).

OligoG CF-5/20 affects cell-signaling in pseudomonal biofilms

To determine whether OligoG CF-5/20 affected these changes via modification of QS signaling in the biofilm systems, liquid chromatography/mass spectrometry (LC/MS) was employed to detect the pseudomonal signaling molecules, C4- and 3-oxo-C12-acyl homoserine lactones (AHLs). AHL levels were determined at 30 and 48 h for PAO1 cells grown in both MH and AS medium. Initial experiments compared growth in MH and AS medium at 30 h (as at earlier time points in AS medium, AHLs were at the limits of detection; results not shown). LC/MS values indicated a reduction in the production of both 3-oxo-C12-AHL and C4-AHL signaling molecules in AS medium (62 and 783 fold respectively) compared to MH medium (**Fig. 4B**). Further experiments were performed on OligoG CF-5/20-treated cultures grown in AS medium for 30 and 48 h (corresponding to mid- and late-stationary phase respectively; results not shown). Interestingly, in this model it was evident that OligoG CF-5/20 (0.2-2%) induced a dose-dependent decrease in 3-oxo-C12 AHL (produced by the Las pathway) in comparison to the control at 30 and 48 h (**Fig. 4C**), but did

not induce any significant change in C4-AHL (produced by the RhlI pathway; **Fig. 4D**). Although OligoG CF-5/20 had a significant effect on biofilm formation, there was no marked difference in ATP production (cell viability) by PAO1 or NH57388A following treatment (**Fig. 4E and 4F**).

The antibiotic properties of colistin were retained in artificial sputum medium when combined with OligoG CF-5/20

Assays of biofilm disruption in established (24 h) non-mucoid (PAO1) and mucoid (NH57388A) pseudomonal biofilms following 24 h treatment with OligoG CF-5/20 and/or colistin were investigated in AS medium. The observed MIC value for colistin was 4x greater in AS medium (0.4 μg/ml versus 0.1 μg/ml) compared to MH medium. The MIC employed in subsequent studies was based upon these findings.

As observed previously, PAO1 and NH57388A demonstrated the formation of large numbers of spherical microcolonies, with extensive EPS in this model (**Fig. 5A, 5B**). The mucoidal NH57388A biofilms were characterized by smaller microcolonies when compared to PAO1 (median diameter 11 μm versus 14 μm respectively) (**Fig. 5C, 5D)**. Biofilm treatment with colistin (at x4 the MBEC value (32), induced disruption of PAO1 and NH57388A bacterial networks. The microcolonies, however, remained intact (with no change in median diameter; $p>0.05$). In contrast, treatment with 2% OligoG CF-5/20 induced significant decreases in the median microcolony diameter (6.9 ±2.0 μm and 6.1 ±2.7 μm; PAO1 and NH57388A respectively; $p<0.05$) characterized by marked disruption of the inter-colony networks and microcolony morphology. Combining OligoG CF-5/20 with colistin (although not as effective as OligoG CF-5/20 alone on the mucoid strain) effectively disrupted both microcolony structure (reducing the median diameter by 60% in PAO1) as well as the inter-colony branching/bridging in both mucoid and non-mucoid models. Overall structural differences can be seen at a lower magnification in **Fig. S2.**

DISCUSSION

The improved survival of CF patients, due in part to the chronic administration of antibiotics, has compounded the problems associated with resistance to antibiotic treatment (35, 36). With the rapid emergence of antibiotic resistance, the development of new therapies is essential. Increased antibiotic resistance in biofilms has been extensively described, with biofilms shown to resist antibiotics by up to 1000 fold (37). These studies demonstrate the potential benefits of combination therapies using a novel mucolytic alongside conventional antibiotics in the treatment of antibiotic-resistant, microcolony-forming *Pseudomonas* sp. lung Infections.

The resurgence of interest in colistin, a highly-effective membrane-permeabilizing antibiotic, reflects the failure of conventional antibiotics in MDR infections (25). Unfortunately, the emergence of plasmid-mediated colistin resistance provides the imminent possibility for horizontal gene transfer from veterinary to human pathogens (38). Due to the high rate of MDR in *P. aeruginosa* (39) colistin is now regarded as an antibiotic of 'last resort' and its use (in non-CF patients) is therefore limited to prevent further development of resistance (40).

Colistin acts through positively-charged electrostatic interactions with the negatively-charged bacterial lipopolysaccharide (LPS), facilitating membrane disruption. The observed lowering of the efficacy of colistin in AS medium may, therefore, not only relate to an altered growth rate in this environment, (which mimics growth conditions in the CF lung), but also may be due to LPS modification and/or direct binding by mucin in the AS medium, effectively 'sequestering' free antibiotic (41). This EPS effect, and the apparent differences in MIC for colistin-treated NH57388A, (with MIC values being 4X greater in AS versus MH medium) reflect the 10^4-fold difference previously observed between MIC (0.094 μg/ml) and MBEC (>512 μg/ml) values for NH57388A *in vitro* (42).

Within the diseased CF lung, >95% of *P. aeruginosa* exist in dense microcolonies, >5 μm from the epithelial cell-surface and independent of cell-surface attachment (14, 43). The microcolonies develop in the early stages of lung infection and readily resist physical disruption (43). The AS medium employed here induced pseudomonal microcolony formation in both non-mucoid and mucoid strains as seen previously. These microcolonies resembled those observed in a range of CF epidemic and non-epidemic *P. aeruginosa* strains (16); SEM demonstrating bridges between the microcolonies which appeared to be composed of elongated single-cells encased in EPS, as previously observed in flow-cell systems (44). OligoG CF-5/20 was able to modulate both the size and structure of these bacterial microcolonies. This may relate to its ability to interact with the EPS component of the biofilm, by direct effects on the pseudomonal bacterial cell-surface, and on bacterial growth (29, 30). Whilst imaging studies demonstrated that colistin effectively disrupted the inter-colony bridges, the microcolonies (which were encased in EPS) appeared unaffected by colistin alone.

Despite the possible charge interactions between the cationic peptide colistin (41) and the anionic OligoG CF-5/20 (30), colistin retained its antibiotic activity in the presence of OligoG CF-5/20. The ability of OligoG CF-5/20 to modify biofilm assembly in *Pseudomonas* spp. has previously been attributed to irreversible binding at the bacterial cell surface (30). Moreover, the ability of OligoG CF-5/20 to potentiate the effectiveness of colistin against mucoid NH57388A biofilms by OligoG CF-5/20 has recently been demonstrated in MBEC assays (32).

In this model, the ability of OligoG CF-5/20 (both alone, and more markedly with colistin) to effectively disrupt the EPS of established biofilms was clearly evident. Disruption of the tight EPS-network, which comprises >90% of the biofilm dry-weight (45), has been shown to lead to less mechanically-stable biofilms, which are then more susceptible to antibiotics (46). It appears therefore that EPS disruption by OligoG CF-5/20 maintained the antimicrobial action of colistin by reducing its ability to bind to components of the biofilm

299 matrix, thereby increasing its penetration through the biofilm, facilitating access of colistin to
300 the pseudomonal cell membrane.

301 Initial experiments demonstrated the contrasting growth phenotype between freshly
302 isolated clinical strains compared to the well-characterized reference strains. Compensatory
303 mutations in the clinical CF isolates are thought to provide differential fitness benefits, which
304 are advantageous within the CF lung environment (47). Fitness 'trade-offs', where beneficial
305 adaptations that improve fitness under one environmental condition that may lead to
306 compensatory loss of other traits have been described (48). This may, in part, explain the
307 observed lower growth rate of fresh clinical isolates (adapted to the CF lung) when
308 compared to the laboratory-maintained IPARP CF strains. This variability highlights the
309 importance of utilizing the reference strain collection for therapeutic development to ensure
310 global standardization of *in vitro* testing.

311 A number of approaches have been attempted to modify biofilm EPS and facilitate
312 treatment or displacement therapy. These have included: use of bacterial polysaccharides
313 e.g. from marine *Vibrio* sp. (49); co-administration of alginate lyase with DNase, which has
314 been reported to increase the efficacy of antibiotics in reducing biofilm growth (50) and co-
315 administration of antibiotics with alginate lyase to eliminate mucoid variants not affected by
316 antibiotics alone (51). Interestingly, we have also previously demonstrated synergy between
317 OligoG CF-5/20 and rhDNase I in modifying the mechanical and structural properties of CF
318 sputum (31).

319 Biofilms also contain bacterially-derived alginates which, in contrast to OligoG CF-5/20,
320 lack G-blocks and have a considerably higher molecular mass (52). Anionic EPS
321 components, such as carboxyl groups, interact strongly with multivalent cations such as
322 Ca^{2+}, resulting in robust biofilms (53). Sletmoen et al., (2012) demonstrated that alginate
323 oligomers may destabilize the interaction between high Mw bacterially-produced alginates
324 and mucin. The ionic displacement of divalent cations e.g. Ca^{2+} has been described as a
325 mechanism by which antimicrobial cationic peptides can potentiate antibiotics (54).
326 Similarly, the anionic alginate G-blocks may displace divalent cations associated with the

biofilm, resulting in a weaker biofilm structure. CD spectroscopy has previously been used to investigate the structural and conformational changes of polysaccharides containing uronic acid residues, and has recently been employed to characterize homopolymeric fractions of the linear co-polymers L-guluronate and D-mannuronate (34, 55). The gelation of alginate in the presence of divalent cations such as Ca^{2+} in homopolyguluroinc acid is known to induce changes in the coordination of the carboxylate groups (56). However, CD spectra indicated that the orientation of the carboxy groups monitored at ~210 nm were not changed upon mixing OligoG CF-5/20 with high Mw alginate.

Previous studies in planktonic systems demonstrated that OligoG CF-5/20 modified both *pilE* gene expression and bacterial motility in *Pseudomonas aeruginosa* (30), which are controlled by QS. The finding that levels of *P. aeruginosa* AHL signaling molecules were significantly reduced in AS medium compared to MH medium was perhaps unsurprising, reflecting the change in growth/morphology. Sriramulu et al (2005), demonstrated the importance of *lasR* for the formation of the dense microcolony phenotype and these data demonstrated the ability of ($\geq$2%) OligoG CF-5/20 to significantly reduce 3-oxo-C12-AHL production at both mid- and late-stationary phase growth (30 and 48 h). The lack of an observed effect on the Rhl product, C4-AHL, may reflect the reduced expression of *rhlR* which is known to occur in AS medium (16).

These experiments demonstrate that the previously described antibacterial effects of OligoG CF-5/20, are evident in this pseudomonal microcolony assay system which more closely resembles growth in the CF lung. It must be remembered that many of the components of the *in vivo* lung are absent in the biofilm model, including lactoferrin, lipids and oligopeptides, which may modulate bacterial behavior *in vivo*. OligoG CF-5/20 was shown to disrupt the biofilm EPS network and, in combined respiratory therapies, this inhaled treatment may facilitate increased access of therapeutic agents to bacteria and/or the lung cell-surface. The mechanistic studies showed that this disruption of EPS structure was not simply related to interaction between the OligoG CF-5/20 and the pseudomonal (M-block alginate), but may rather reflect modification of QS signaling within the biofilm. The

findings here, and the proven safety of the agent as an inhalational therapy (www.clinicaltrials.gov, Identifier: NCT00970346 and NCT01465529), highlight the potential utility of this agent in the treatment of MDR bacterial infections in a range of human diseases. Phase IIb human studies are currently ongoing (www.clinicaltrials.gov, Identifier: NCT02157922 and NCT02453789).

METHODS

Bacterial strains and media

P. aeruginosa strains were cultured on blood agar plates and grown overnight in Tryptone soy broth (TSB; LabM), at 37°C. Mueller Hinton (MH) medium or Artificial Sputum (AS) medium (adapted from earlier studies [43] by supplementation with 20 ml/L RPMI 1640 as an amino acid source; Sigma Aldrich) were also employed.

Reference strains (n=7) were obtained from the International *P. aeruginosa* Reference Panel (IPARP) (57) including: AA2 and AA44 (early and late non-mucoid CF colonizers respectively); AA43 (mucoidal colonizer from the same AT code) and mucoidal CF isolates, IST 27 (Lisbon, Portugal) and 2192 (source ID; Boston, MA). The well characterized non-mucoid PAO1 and mucoidal MDR CF strain NH57388A (Copenhagen, Denmark), were also used in subsequent experiments.

Patients and clinical isolates

Newly isolated, non-mucoid *P. aeruginosa* strains (22078, 22554, and 22476) were obtained from induced sputum collected from children attending the Cystic Fibrosis Unit at the University Hospital of Wales, Cardiff participating in the Sputum Induction Trial (SpIT) study (a longitudinal sputum collection study in CF patients; LREC approved [project ID 11/RPM/5216]).

Changes in antibiotic susceptibility in the different media

Bacteriocidal values for colistin in MH and AS medium were studied using standard minimum inhibitory concentration (MIC) assays as previously described (29).

Effects of OligoG CF-5/20 on pseudomonal growth in the presence of colistin

For the inoculum for the pseudomonal growth curves, overnight cultures in TSB (n=3) were standardized to 10^6 cells/ml in MH medium. For treated samples, *P. aeruginosa* (NH57388A; n=3) standardized to 10^8 cells/ml in MH medium were treated with and without 2% OligoG CF-5/20 (w/v) ± colistin (0.5x MIC; 0.05 µg/ml). Samples were grown (24 h; 37°C) in 96-well plates and change in cell density recorded every hour (OD_{600}) on a FLUOstar Omega plate reader. Cell doubling time was calculated for each growth curve.

Viable microbial cell numbers in culture when treated with OligoG CF-5/20

Adenosine triphosphate (ATP) production by PAO1 and NH57388A was compared in MH and AS medium ± 2% OligoG CF-5/10. Cultures were prepared as for the growth curve experiments and analyzed using the BacTiter-Glo™ Microbial Cell Viability Assay (Promega) at 0, 2, 4, 6, 8, 12, 24 and 48 h with luminescence read on a FLUOstar Omega plate reader.

Confocal laser scanning microscopy biofilms in MH and AS media in the presence of OligoG CF-5/20

Pseudomonal cultures (NH57388A) standardized to 10^7 cfu/ml, were inoculated 1:20 in MH or AS media and incubated (37°C; 20 rpm) for 24 h or 48 h respectively in Greiner glass-bottomed optical 96-well plates; the difference in growth rates in the two media, accounting for the longer growth time used for the AS medium. For antimicrobial treatment, half of the supernatant was gently removed and replaced with fresh MH or AS medium ± 2% OligoG CF-5/20 and/or colistin at half the MBEC (2 µg/ml) and incubated for 1 h.

Supernatant was then removed and replaced with 6% (v/v) LIVE/DEAD® (Invitrogen) stain in PBS prior to imaging. CLSM was performed using a Leica SP5 confocal microscope with x63 magnification under oil. Z-stack CLSM images were analyzed using COMSTAT image analysis software (33).

AS medium biofilms were also fixed overnight at 4°C with 3% (v/v) glutaraldehyde and stained (1 h) at room temperature with 0.15% Syto-9 (Invitrogen) in PBS. CLSM of Z-stack images was achieved using sequential fluorescence recordings of Syto-9 ($\lambda_{ex}/\lambda_{em}$ max: $480/500_{nm}$) and propidium iodide ($\lambda_{ex}/\lambda_{em}$ max: $490/635_{nm}$).

For EPS imaging, NH57388A biofilms (48 h) were grown in AS medium in 12-well glass bottomed plates (No. 1.5; MatTek Corp. Ashland, MA, USA) ± 2 or 6% OligoG CF-5/20.. Biofilms were fixed with 2.5% glutaraldehyde in PBS overnight at 4°C. Fixative was then removed and biofilms stained with Syto-9 (0.15% in PBS) and Concanavalin A, Alexa Fluor™ 633 Conjugate (100 μg/ml in PBS; Invitrogen) prior to CLSM imaging.

Scanning electron microscopy of OligoG CF-5/20 treated biofilms in different media

P. aeruginosa (PAO1 and NH57388A) cultures were adjusted to 10^7 cfu/ml in MH or AS medium and grown (37°C for 24 h or 48 h respectively at 20 rpm) in 12-well plate (Greiner Bio-One) on Thermanox™ glass slides (Agar Scientific) ± OligoG CF-5/20 0.2%, 2% or 6% (w/v). For the established (24 h) biofilm model, half the supernatant was gently removed and replaced with 2% OligoG CF-5/20 (v/v), colistin (x4 MBEC; 16 μg/ml), or combination treatment and incubated for 24 h. Supernatant was removed and biofilms fixed with 2.5% (v/v) glutaraldehyde prior to being washed (x4) with dH_2O and freeze-dried. The samples were then gold-coated and imaged using a Tescan Vega conventional SEM (2.5 kV) for untreated samples and the established biofilm model or performed using a Hitachi S4800 (1 kV) scanning electron microscope (SEM) for the biofilm development model. Pseudo-coloring of SEM images was performed using Adobe Photoshop CS6 (Adobe Systems

Europe Ltd, Maidenhead, UK). ImageJ was used to measure microcolony diameter following line calibration using the known set scale for each image. Measurements of the three largest cellular aggregates in each image were taken at the narrowest diameter.

Direct interaction of OligoG CF-5/20 and pseudomonal high molecular weight alginate using circular dichroism spectroscopy

CD spectra of OligoG CF-5/20, high Mw alginate (approx. 100 kDa) comprising 7% guluronic acid derived from *Pseudomonas aeruginosa*, and mixtures thereof were recorded using an Aviv Model 215 instrument (Aviv Biomedical, Lakewood, NJ, U.S.A.). Samples were dissolved in 100 mM NaCl, 5 mM Tris.Cl, pH 7.5, spun at 14,000 *g* for 30 min at 4°C, and the supernatant transferred to a 0.1-cm quartz cell pre-warmed to 37°C. Repetitive spectra were collected from 245 to 196 nm at 0.2 nm intervals with 2 s accumulation per point corresponding to ~11 min/spectrum). Buffer baselines were subtracted and ellipticities (Θ) were corrected for dilutions.

Changes in quorum sensing acyl-homoserine lactone (AHL) production in different media when treated with OligoG CF-5/20

Overnight cultures of *P. aeruginosa* PAO1 were diluted (1:100) in either MH or AS medium and grown for a further 30 or 48 h ± 0.2 or 2 % OligoG CF-5/20. Cultures were washed (x3; 18,000 *g*, 20 min, 4°C) in ice cold 0.9% NaCl and pelleted cells were dried (80°C) for 24 h and weighed. Culture supernatants were vigorously mixed (30 s) in equal volumes of ethyl acetate (acidified with 0.5% formic acid), and the upper layer collected (x3). The resultant ethyl acetate fractions were allowed to evaporate and the precipitate was re-suspended in 1 ml of distilled H_2O (58). Samples were freeze-dried prior to analysis. Quantification of acyl

458 homoserine lactones was done using high performance liquid chromatography triple
459 quadrupole mass spectrometry (LC-QQQ-MS).
460 Freeze-dried samples were maintained on ice and reconstituted in acetonitrile (200
461 µl) with 0.1% acetic acid and 7.2 ng ml^{-1} of the internal standard umbelliferone. Samples
462 were centrifuged (16,100 *g*, 10 min, 4°C) and supernatants filtered (0.4 µm; x2). Samples (5
463 µl) were loaded onto a C18 XDB Eclipse (1.8 µm, 4.6 x 50 mm) reverse phase column and
464 quantified using a 1200 series HPLC coupled to a 6410B enhanced sensitivity triple
465 quadrupole (QQQ) mass spectrometer (Agilent Technologies, Palo Alto, USA). For
466 detection using positive ion mode, mobile phase A comprised of 5 mM ammonium acetate in
467 water modified with 0.1% acetic acid and B was acetonitrile containing 0.1% acetic acid.
468 The column was equilibrated in 2% B before increasing in a linear fashion to 100% over 6
469 mins. 100% B was maintained for a further 2 min before column re-equilibration. The
470 column temperature was maintained at 35°C for the duration with a flow rate of 0.3 mL/min.
471 Source parameters were set as follows: Temperature, 350°C; gas flow, 10 L/min; nebulizer,
472 35 psi; and capillary voltage, 4 kV. Data was analysed using Agilent MassHunter QQQ
473 Quantitative Analysis software (Version B.07.00). Peak areas were normalized to the
474 internal standard umbelliferone and concentrations calculated using standard concentration
475 curves, offset against blank values (the average peak areas for the blanks).

476

477 **Statistical analysis**

478 The COMSTAT data was normally distributed so a standard t-test was performed using
479 MiniTab 17 (Minitab Ltd, Coventry, UK) and a Bonferroni correction. A one-way ANOVA was
480 used for the AHL data using GraphPad 3 (La Jolla, CA, USA). STATA was used to carry out
481 a Kruskal-Wallis non-parametric test supplemented using Dunn's test for the microcolony
482 SEM measurements.

483

ACKNOWLEDGEMENTS

This study was supported by funding from the European Union via the Eurostars (TM) Programme and the European Social Fund, Research Council of Norway, Cystic Fibrosis Foundation US and AlgiPharma AS. We thank Professor N. Høiby for *P. aeruginosa* strain NH57388A and Debbie Salmon for technical support for the LC/MS. We thank Professor Gudmund Skjåk-Bræk for providing the high Mw pseudomonal alginate for the CD studies. We would also like to thank Dr Damian Farnell for his support with the statistical analysis. D.W.T. has a consultancy relationship and has, with K.E.H., received research funding from AlgiPharma AS. A.D and P.D.R. are director/owners of AlgiPharma AS. The other authors have no conflicts of interest to disclose.

FIGURE LEGENDS

FIG 1 Comparison of planktonic growth in MH medium of characterized and new cystic fibrosis *P. aeruginosa* isolates and biofilm growth following antimicrobial treatment. Growth curves (24 h) of (A) Non-mucoid IPARP isolates (red) versus fresh clinical SpIT isolates (blue) and (B) non-mucoid IPARP isolates (red) versus mucoid (green). (C) Growth curves of NH57388A (36 h) ± 2% and OligoG CF-5/20 with/without colistin (0.05 μg/ml). Biofilm disruption assay showing LIVE/DEAD® CLSM [scale bar 20 μm] of 24 h established NH57388A biofilms, (D) untreated control, (E) 1 h colistin treatment, (F) 2% OligoG CF-5/20, (G) combined treatment. COMSTAT analysis showing (H) mean height of biofilm and (I) ratio of DEAD: LIVE cells. (*$p<0.05$)

FIG 2 Comparison of growth of non-mucoid PAO1 and mucoid NH57388A *P. aeruginosa* in Mueller-Hinton (MH) and artificial sputum (AS) medium. Scanning electron microscopy of bacterial growth in MH (24 h) and AS medium (48 h; scale bar 20 μm), with corresponding 'zoomed-in' images in AS medium [scale bar 10 μm] (A) PAO1 and (B) NH57388A. (C)

510 Diagrammatic representation of biofilm structure in both media. (D) Cell viability (ATP
511 production) of *P. aeruginosa* NH57388A and PAO1 (10^8 cfu/ml) grown in MH and AS
512 medium.
513
514 **FIG 3** Biofilm formation assays showing mucoid NH57388A *P. aeruginosa* biofilms grown in
515 Mueller-Hinton (MH) and artificial sputum (AS) medium. SEM images of *P. aeruginosa*
516 (NH57388A) biofilms grown ±OligoG CF-5/20 for (A) 24 h in Mueller Hinton (MH) medium;
517 10 µm; (B), (C [zoomed in]) 48 h ± OligoG CF-5/20 [scale bar 5 µm] with (D) corresponding
518 scatter graphs showing approx. mean microcolony size. (E) Corresponding CLSM EPS
519 staining of *P. aeruginosa* (NH57388A) 48 h biofilms in artificial sputum (AS) medium using
520 Syto-9 (green) and Concanavalin A 633 (red). (F,G) Biofilm disruption assay using Syto-9
521 (green) showing cross-sectional views of 48 h established biofilms treated l h with 2%
522 OligoG CF-5/20 [scale bar 10 µm]. (*p<0.05).
523
524 **FIG 4** Effect of OligoG CF-5/20 on high Mw alginate and on cell signaling molecules *in vitro*.
525 (A) Circular dichroism (CD) spectra of high Mw pseudomonal alginate mixed with OligoG
526 CF-5/20. Scans 1-7 show spectra of high Mw alginate (~20 µM) followed over ~77 min upon
527 heating from 4 to 37^0C; scans 8-11 (~44min) are recorded after addition of OligoG CF-5/20
528 (850 µM) followed by addition of Ca^{2+} (1mM) (scans 12-17, ~ 66min). Spectra of OligoG CF-
529 5/20 (850 µM) alone and its sum with high Mw alginate (20 µM) are shown as black and red
530 dashed lines, respectively. High performance liquid chromatography (HPLC) mass
531 spectrometry (LC-QQQ-MS) to quantify acyl homoserine lactone (AHL; 3-oxo-C12-AHL and
532 C4-AHL) production of *P. aeruginosa* PAO1 (B) grown in MH and AS medium (30 h), and in
533 a time course assay (30 and 48 h) showing the effect of OligoG CF-5/20 on (C) 3-oxo C12-
534 AHL and (D) C4-AHL (*p<0.05; n=3). Cell viability (ATP production) over 48 h of (E) PAO1
535 and (F) NH57388A grown in MH and AS medium ± 2% OligoG CF-5/20 (2%G).
536

FIG 5 Biofilm disruption assays showing scanning electron microscopy (SEM) of antimicrobial (OligoG CF 5/20 and colistin) treated biofilms grown in ASM [Scale bar 10 μm]. SEM images of established (24 h) *P. aeruginosa* (A) PAO1 and (B) NH57388A biofilms treated for 24 h with 2% OligoG CF-5/20 ± colistin (16 μg/ml) with corresponding median microcolony diameter measurements for (C) PAO1 and (D) NH57388A (*p<0.05).

Supplementary Figures

FIG S1 CD spectra of high Mw pseudomonal alginate mixed with OligoG CF-5/20. Scans 1-2 show spectra of high Mw alginate (~20 μM) followed over ~22 min after heating from 4 to 37°C, after which Ca^{2+} was added (scans 3-8: c_{final} = 1mM; scans 9-11: c_{final} = 2mM). Oligo G CF-5/20 was added to c_{fin} = 700μM (scans 12-15; molar ratio high Mw alginate to OligoG CF-5/20 1:50) and c_{fin} = 4.2mM (scans 16-22; molar ratio high Mw alginate to OligoG CF-5/20 1:600). Adding calcium to c_{fin} = 9 mM results in spontaneous alginate precipitation (scans 23-25).

FIG S2 Biofilm disruption assay showing SEM images of established (24 h) *P. aeruginosa* (A) PAO1 and (B) NH57388A biofilms treated for 24 10 h with 2% OligoG CF-5/20 ± colistin (16 μg/ml). Scale bar 20 μm.

REFERENCES

1. Valderrey AD, Pozuelo MJ, Jimenez PA, Macia MD, Oliver A, Rotger R. 2010. Chronic colonization by *Pseudomonas aeruginosa* of patients with obstructive lung diseases: cystic fibrosis, bronchiectasis, and chronic obstructive pulmonary disease. Diagn Microbiol Infect Dis 68:20-27.
2. Farrell PM. 2008. The prevalence of cystic fibrosis in the European Union. J Cyst Fibros 7:450-453.

563 3. Rubin BK. 2009. Mucus, phlegm, and sputum in cystic fibrosis. Respir Care 54:726-
564 732.
565 4. Li ZH, Kosorok MR, Farrell PM, Laxova A, West SEH, Green CG, Collins J, Rock MJ,
566 Splaingard ML. 2005. Longitudinal development of mucoid *Pseudomonas aeruginosa*
567 infection and lung disease progression in children with cystic fibrosis. JAMA 293:581-
568 588.
569 5. Marvig RL, Johansen HK, Molin S, Jelsbak L. 2013. Genome analysis of a
570 transmissible lineage of *Pseudomonas aeruginosa* reveals pathoadaptive mutations
571 and distinct evolutionary paths of hypermutators. Plos Genet 9,
572 doi:10.1371/journal.pgen.1003741.
573 6. Feliziani S, Marvig RL, Lujan AM, Moyano AJ, Di Rienzo JA, Johansen HK, Molin S,
574 Smania AM. 2014. Coexistence and within-host evolution of diversified lineages of
575 hypermutable *Pseudomonas aeruginosa* in long-term cystic fibrosis infections. Plos
576 Genet 10, doi:10.1371/journal.pgen.1004651.
577 7. Marvig RL, Sommer LM, Molin S, Johansen HK. 2015. Convergent evolution and
578 adaptation of *Pseudomonas aeruginosa* within patients with cystic fibrosis. Nature
579 Genet 47:57-64.
580 8. Bales PM, Renke EM, May SL, Shen Y, Nelson DC. 2013. Purification and
581 characterization of biofilm-associated EPS exopolysaccharides from ESKAPE
582 organisms and other pathogens. Plos One 8, doi:10.1371/journal.pone.0096166.
583 9. Ryall B, Carrara M, Zlosnik JEA, Behrends V, Lee X, Wong Z, Lougheed KE,
584 Williams HD. 2014. The mucoid switch in *Pseudomonas aeruginosa* represses
585 quorum sensing systems and leads to complex changes to stationary phase
586 virulence factor regulation. Plos One 9, doi:10.1371/journal.pone.0096166.
587 10. Ryall B, Davies JC, Wilson R, Shoemark A, Williams HD. 2008. *Pseudomonas*
588 *aeruginosa*, cyanide accumulation and lung function in CF and non-CF
589 bronchiectasis patients. Eur Resp J 32:740-747.

590 11. Leid JG, Willson CJ, Shirtliff ME, Hassett DJ, Parsek MR, Jeffers AK. 2005. The
591 exopolysaccharide alginate protects *Pseudomonas aeruginosa* biofilm bacteria from
592 IFN-gamma-mediated macrophage killing. J Immunol 175:7512-7518.
593 12. Waine DJ, Honeybourne D, Smith EG, Whitehouse JL, Dowson CG. 2008.
594 Association between hypermutator phenotype, clinical variables, mucoid phenotype,
595 and antimicrobial resistance in *Pseudomonas aeruginosa*. J Clin Microbiol 46:3491-
596 3493.
597 13. Cystic fibrosis patient registry annual report 2014. Available from:
598 https://www.cff.org/2014-Annual-Data-Report.pdf.
599 14. Worlitzsch D, Tarran R, Ulrich M, Schwab U, Cekici A, Meyer KC, Birrer P, Bellon G,
600 Berger J, Weiss T, Botzenhart K, Yankaskas JR, Randell S, Boucher RC, Doring G.
601 2002. Effects of reduced mucus oxygen concentration in airway *Pseudomonas*
602 infections of cystic fibrosis patients. J Clin Invest 109:317-325.
603 15. Kirchner S, Fothergill JL, Wright EA, James CE, Mowat E, Winstanley C. 2012. Use
604 of artificial sputum medium to test antibiotic efficacy against *Pseudomonas*
605 *aeruginosa* in conditions more relevant to the cystic fibrosis lung. J Vis Exp
606 doi:10.3791/3857.
607 16. Fung C, Naughton S, Turnbull L, Tingpej P, Rose B, Arthur J, Hu H, Harmer C,
608 Harbour C, Hassett DJ, Whitchurch CB, Manos J. 2010. Gene expression of
609 *Pseudomonas aeruginosa* in a mucin-containing synthetic growth medium mimicking
610 cystic fibrosis lung sputum. J Med Microbiol 59:1089-1100.
611 17. Quinn RA, Whiteson K, Lim Y-W, Salamon P, Bailey B, Mienardi S, Sanchez SE,
612 Blake D, Conrad D, Rohwer F. 2015. A Winogradsky-based culture system shows an
613 association between microbial fermentation and cystic fibrosis exacerbation. ISME J
614 9:1024-1038.
615 18. McCarthy RR, Mooij MJ, Reen FJ, Lesouhaitier O, O'Gara F. 2014. A new regulator
616 of pathogenicity (bvlR) is required for full virulence and tight microcolony formation in
617 *Pseudomonas aeruginosa*. Microbiol 160:1488-1500.

19. Windmueller N, Witten A, Block D, Bunk B, Sproeer C, Kahl BC, Mellmann A. 2015. Transcriptional adaptations during long-term persistence of *Staphylococcus aureus* in the airways of a cystic fibrosis patient. International J Med Microbiol 305:38-46.
20. Nafee N, Husari A, Maurer CK, Lu C, de Rossi C, Steinbach A, Hartmann RW, Lehr C-M, Schneider M. 2014. Antibiotic-free nanotherapeutics: Ultra-small, mucus-penetrating solid lipid nanoparticles enhance the pulmonary delivery and anti-virulence efficacy of novel quorum sensing inhibitors. J Control Release 192:131-140.
21. Yang Y, Tsifansky MD, Wu CJ, Yang HI, Schmidt G, Yeo Y. 2010. Inhalable antibiotic delivery using a dry powder co-delivering recombinant deoxyribonuclease and ciprofloxacin for treatment of cystic fibrosis. Pharm Res 27:151-160.
22. Nguyen D, Joshi-Datar A, Lepine F, Bauerle E, Olakanmi O, Beer K, McKay G, Siehnel R, Schafhauser J, Wang Y, Britigan BE, Singh PK. 2011. Active starvation responses mediate antibiotic tolerance in biofilms and nutrient-limited bacteria. Science 334:982-986.
23. Filkins LM, O'Toole GA. 2015. Cystic fibrosis lung infections: polymicrobial, complex, and hard to treat. Plos Path 11, doi:10.1371/journal.ppat.1005258.
24. Barry PJ, Jones AM. 2015. New and emerging treatments for cystic fibrosis. Drugs 75:1165-1175.
25. Li J, Nation RL, Turnidge JD, Milne RW, Coulthard K, Rayner CR, Paterson DL. 2006. Colistin: the re-emerging antibiotic for multidrug-resistant Gram-negative bacterial infections. Lancet Infect Dis 6:589-601.
26. Azzopardi EA, Ferguson EL, Thomas DW. 2013. The enhanced permeability retention effect: a new paradigm for drug targeting in infection. J Antimicrob Chemother 68:257-274.
27. Li J, Nation RL, Milne RW, Turnidge JD, Coulthard K. 2005. Evaluation of colistin as an agent against multi-resistant in Gram-negative bacteria. Int J Antimicrob Agents 25:11-25.

646 28. Barriere SL. 2015. Clinical, economic and societal impact of antibiotic resistance.
647 Expert Opin Pharmacother 16:151-153.
648 29. Khan S, Tondervik A, Sletta H, Klinkenberg G, Emanuel C, Onsøyen E, Myrvold R,
649 Howe RA, Walsh TR, Hill KE, Thomas DW. 2012. Overcoming drug resistance with
650 alginate oligosaccharides able to potentiate the action of selected antibiotics.
651 Antimicrob Agents Chemother 56:5134-5141.
652 30. Powell LC, Pritchard MF, Emanuel C, Onsøyen E, Rye PD, Wright CJ, Hill KE,
653 Thomas DW. 2014. A nanoscale characterization of the interaction of a novel
654 alginate oligomer with the cell surface and motility of *Pseudomonas aeruginosa*. Am.
655 J Respir Cell Mol Biol 50:483-492.
656 31. Pritchard MF, Powell LC, Menzies GE, Lewis PD, Hawkins K, Wright C, Doull I,
657 Walsh TR, Onsøyen E, Dessen A, Myrvold R, Rye PD, Myrset AH, Stevens HNE,
658 Hodges LA, MacGregor G, Neilly JB, Hill KE, Thomas DW. 2016. A new class of safe
659 oligosaccharide polymer therapy to modify the mucus barrier of chronic respiratory
660 disease. Mol Pharma 13:863-872.
661 32. Hengzhuang W, Song Z, Ciofu O, Onsøyen E, Rye PD, Høiby N. 2016. OligoG CF-
662 5/20 Disruption of Mucoid *Pseudomonas aeruginosa* Biofilm in a Murine Lung
663 Infection Model. Antimicrob Agents Chemother 60:2620-2626.
664 33. Heydorn A, Nielsen AT, Hentzer M, Sternberg C, Givskov M, Ersboll BK, Molin S.
665 2000. Quantification of biofilm structures by the novel computer program COMSTAT.
666 Microbiol 146:2395-2407.
667 34. Morris ER, Rees DA, Sanderson GR, Thom D. 1975. Conformation and circular
668 dichroism of uronic acid residues in glycosides and polysaccharides. J Chem Soc
669 Perk. 2:1418-1425.
670 35. Ciofu O, Tolker-Nielsen T, Jensen PO, Wang H, Høiby N. 2015. Antimicrobial
671 resistance, respiratory tract infections and role of biofilms in lung infections in cystic
672 fibrosis patients. Adv Drug Deliv Rev 85:7-23.

673 36. Sherrard LJ, Tunney MM, Elborn JS. 2014. Antimicrobial resistance in the respiratory
674 microbiota of people with cystic fibrosis. Lancet 384:703-713.
675 37. Ceri H, Olson ME, Stremick C, Read RR, Morck D, Buret A. 1999. The Calgary
676 Biofilm Device: New technology for rapid determination of antibiotic susceptibilities of
677 bacterial biofilms. J Clin Microbiol 37:1771-1776.
678 38. Liu Y-Y, Wang Y, Walsh TR, Yi L-X, Zhang R, Spencer J, Doi Y, Tian G, Dong B,
679 Huang X, Yu L-F, Gu D, Ren H, Chen X, Lv L, He D, Zhou H, Liang Z, Liu J-H, Shen
680 J. 2016. Emergence of plasmid-mediated colistin resistance mechanism MCR-1 in
681 animals and human beings in China: a microbiological and molecular biological
682 study. Lancet Infect Dis 16:161-168.
683 39. Breidenstein EBM, de la Fuente-Nunez C, Hancock REW. 2011. *Pseudomonas*
684 *aeruginosa*: all roads lead to resistance. Trends in Microbiol 19:419-426.
685 40. Nation RL, Li J, Cars O, Couet W, Dudley MN, Kaye KS, Mouton JW, Paterson DL,
686 Tam VH, Theuretzbacher U, Tsuji BT, Turnidge JD. 2015. Framework for
687 optimisation of the clinical use of colistin and polymyxin B: the Prato polymyxin
688 consensus. Lancet Infect Dis 15:225-234.
689 41. Huang JX, Blaskovich MAT, Pelingon R, Ramu S, Kavanagh A, Elliott AG, Butler MS,
690 Montgomery AB, Cooper MA. 2015. Mucin binding reduces colistin antimicrobial
691 activity. Antimicrob Agents Chemother 59:5925-5931.
692 42. Hengzhuang W, Song Z, Ciofu O, Onsøyen E, Rye P, Høiby N. 2013. Biofilm
693 disruption and synergistic antimicrobial effects of a novel alginate oligomer on
694 *Pseudomonas aeruginosa in vivo*. Pediatr Pulmonol 48:294-294.
695 43. Sriramulu DD, Lunsdorf H, Lam JS, Romling U. 2005. Microcolony formation: a novel
696 biofilm model of Pseudomonas aeruginosa for the cystic fibrosis lung. J Med
697 Microbiol 54:667-676.
698 44. Nivens DE, Ohman DE, Williams J, Franklin MJ. 2001. Role of alginate and its O
699 acetylation in formation of *Pseudomonas aeruginosa* microcolonies and biofilms. J
700 Bacteriol 183:1047-1057.

701 45. Garnett JA, Matthews S. 2012. Interactions in bacterial biofilm development: A
702 structural perspective. Curr Protein Pept Sci 13:739-755.
703 46. Billings N, Millan MR, Caldara M, Rusconi R, Tarasova Y, Stocker R, Ribbeck K.
704 2013. The extracellular matrix component Psl provides fast-acting antibiotic defense
705 in *Pseudomonas aeruginosa* biofilms. Plos Path 9, doi:10.1371/journal.ppat.1003526.
706 47. Caballero JD, Clark ST, Coburn B, Zhang Y, Wang PW, Donaldson SL, Tullis DE,
707 Yau YCW, Waters VJ, Hwang DM, Guttman DS. 2015. Selective sweeps and parallel
708 pathoadaptation drive *Pseudomonas aeruginosa* evolution in the cystic fibrosis lung.
709 mBio 6, doi:10.1128/mBio.00981-15
710 48. Carroll SM, Lee M-C, Marx CJ. 2014. Sign epistasis limits evolutionary trade-offs at
711 the confluence of single- and multi-carbon metabolism in *Methylobacterium*
712 *Extorquens* AM1. Evolution 68:760-771.
713 49. Jiang P, Li J, Han F, Duan G, Lu X, Gu Y, Yu W. 2011. Antibiofilm Antibiofilm activity
714 of an exopolysaccharide from marine bacterium *Vibrio* sp QY101. Plos One 6:1-11.
715 50. Alipour M, Suntres ZE, Omri A. 2009. Importance of DNase and alginate lyase for
716 enhancing free and liposome encapsulated aminoglycoside activity against
717 *Pseudomonas aeruginosa*. J Antimicrob Chemother 64:317-325.
718 51. Alkawash MA, Soothill JS, Schiller NL. 2006. Alginate lyase enhances antibiotic
719 killing of mucoid *Pseudomonas aeruginosa* in biofilms. APMIS 114:131-138.
720 52. Lembre P, Lorentz Cc, Di Martino P. 2012. Exopolysaccharides of the biofilm matrix:
721 A complex biophysical world. INTECH Open Access Publisher, doi: 10.5772/51213.
722 Available from: http://www.intechopen.com/books/the-complex-world-of-
723 polysaccharides/exopolysaccharides-of-the-biofilm-matrix-a-complex-biophysical-
724 world
725 53. Flemming H.C, Wingender J. 2010. The biofilm matrix. Nat Rev Microbiol 8:623-633.
726 54. Aslam SN, Newman MA, Erbs G, Morrissey KL, Chinchilla D, Boller T, Jensen TT,
727 De Castro C, Ierano T, Molinaro A, Jackson RW, Knight MR, Cooper RM. 2008.

728 Bacterial polysaccharides suppress induced innate immunity by calcium chelation.
729 Curr Biol 18:1078-1083.
730 55. Martinez-Gomez F, Mansilla A, Matsuhiro B, Matulewicz MC, Troncoso-Valenzuela
731 MA. 2016. Chiroptical characterization of homopolymeric block fractions in alginates.
732 Carbohydr Polym 146:90-101.
733 56. Grant GT, Morris ER, Rees DA, Smith PJC, Thom D. 1973. Biological interactions
734 between polysaccharides and divalent cations: The egg-box model. FEBS Lett.
735 32:195-198.
736 57. De Soyza A, Hall AJ, Mahenthiralingam E, Drevinek P, Kaca W, Drulis-Kawa Z,
737 Stoitsova SR, Toth V, Coenye T, Zlosnik JEA, Burns JL, Sa-Correia I, De Vos D,
738 Pirnay J-P, Kidd TJ, Reid D, Manos J, Klockgether J, Wiehlmann L, Tuemmler B,
739 McClean S, Winstanley C, BM EFFCA. 2013. Developing an international
740 *Pseudomonas aeruginosa* reference panel. MicrobiologyOpen 2:1010-1023.
741 58. Ravn L, Christensen AB, Molin S, Givskov M, Gram L. 2001. Methods for detecting
742 acylated homoserine lactones produced by Gram-negative bacteria and their
743 application in studies of AHL-production kinetics. J Microbiol Methods 44:239-251.

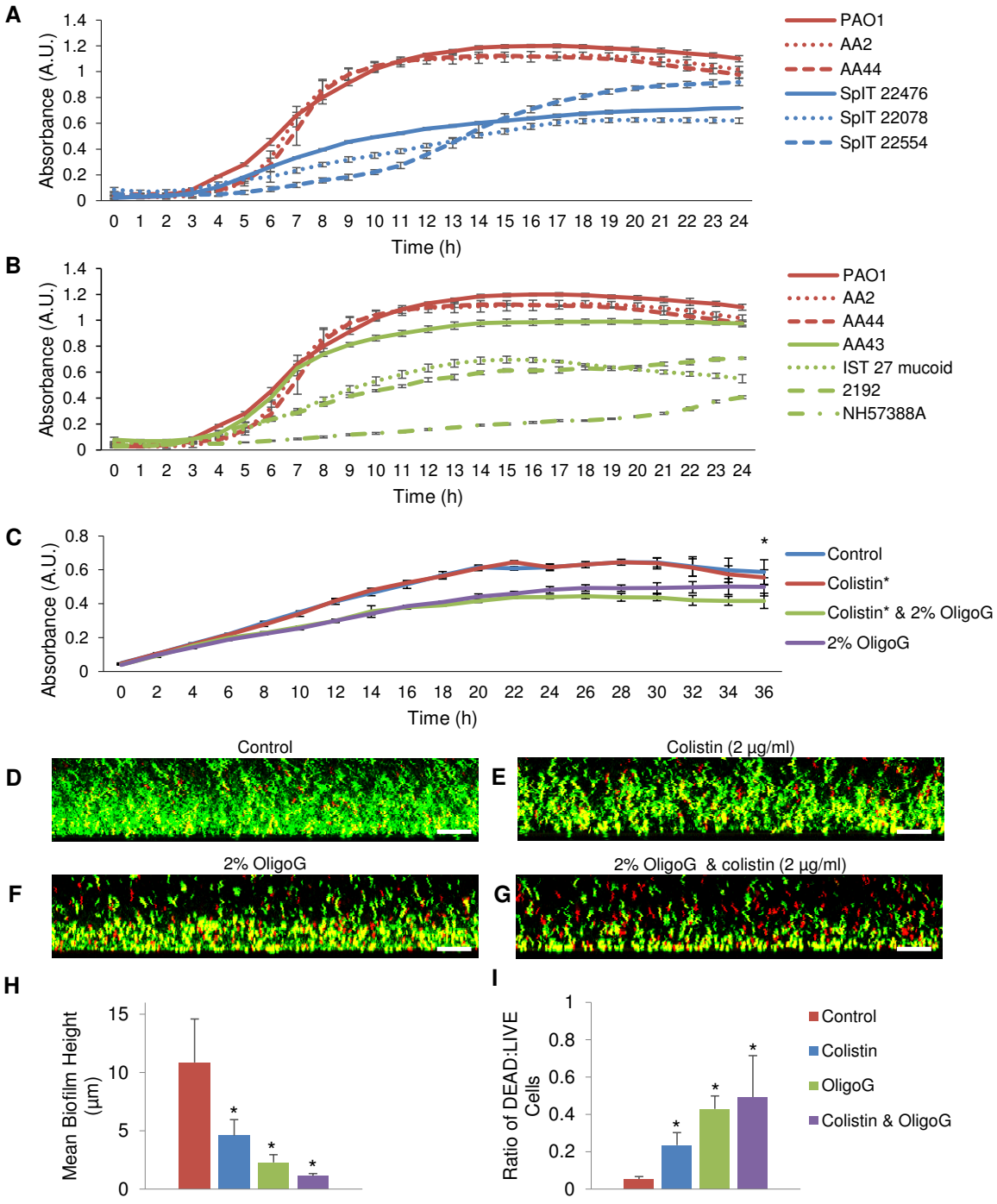

FIG 1 Comparison of planktonic growth in MH medium of characterized and new cystic fibrosis *P. aeruginosa* isolates and biofilm growth following antimicrobial treatment. Growth curves (24 h) of (A) Non-mucoid IPARP isolates (red) versus fresh clinical SpIT isolates (blue) and (B) non-mucoid IPARP isolates (red) versus mucoid (green). (C) Growth curves of NH57388A (36 h) ± 2% and OligoG CF-5/20 with/without colistin (0.05 µg/ml). Biofilm disruption assay showing LIVE/DEAD® CLSM [scale bar 20 µm] of 24 h established NH57388A biofilms, (D) untreated control, (E) 1 h colistin treatment, (F) 2% OligoG CF-5/20, (G) combined treatment. COMSTAT analysis showing (H) mean height of biofilm and (I) ratio of DEAD: LIVE cells. (*p<0.05)

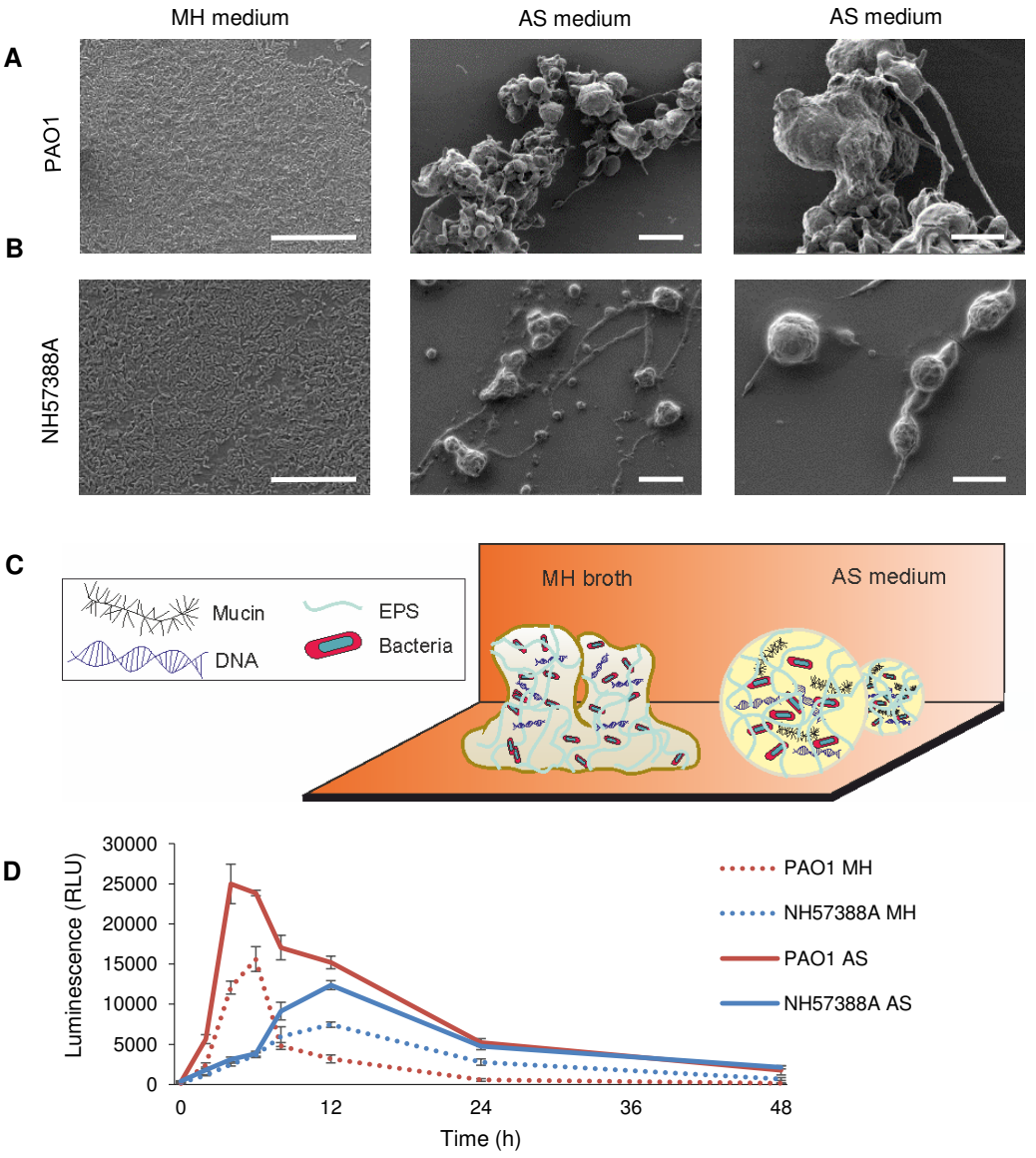

FIG 2 Comparison of growth of non-mucoid PAO1 and mucoid NH57388A *P. aeruginosa* in Mueller-Hinton (MH) and artificial sputum (AS) medium. Scanning electron microscopy of bacterial growth in MH (24 h) and AS medium (48 h; scale bar 20 µm), with corresponding 'zoomed-in' images in AS medium [scale bar 10 µm] (A) PAO1 and (B) NH57388A. (C) Diagrammatic representation of biofilm structure in both media. (D) Cell viability (ATP production) of *P. aeruginosa* NH57388A and PAO1 (10^8 cfu/ml) grown in MH and AS medium.

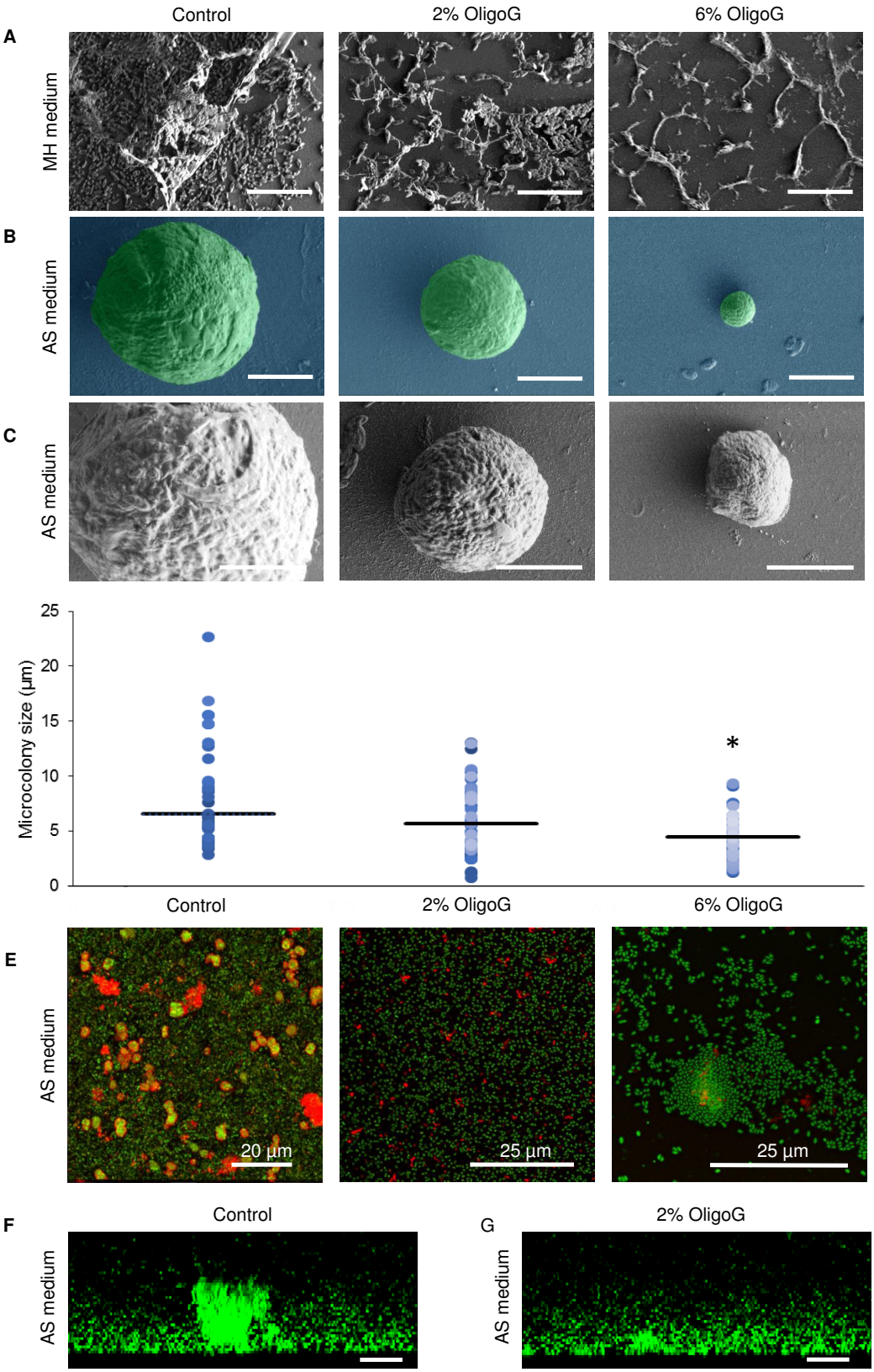

FIG 3 Biofilm formation assays showing mucoid NH57388A *P. aeruginosa* biofilms grown in Mueller-Hinton (MH) and artificial sputum (AS) medium. SEM images of *P. aeruginosa* (NH57388A) biofilms grown ±OligoG CF-5/20 for (A) 24 h in Mueller Hinton (MH) medium; 10 µm; (B), (C [zoomed in]) 48 h ± OligoG CF-5/20 [scale bar 5 µm] with (D) corresponding scatter graphs showing approx. mean microcolony size. (E) Corresponding CLSM EPS staining of *P. aeruginosa* (NH57388A) 48 h biofilms in artificial sputum (AS) medium using Syto-9 (green) and Concanavalin A 633 (red). (F,G) Biofilm disruption assay using Syto-9 (green) showing cross-sectional views of 48 h established biofilms treated I h with 2% OligoG CF-5/20 [scale bar 10 µm]. (*p<0.05).

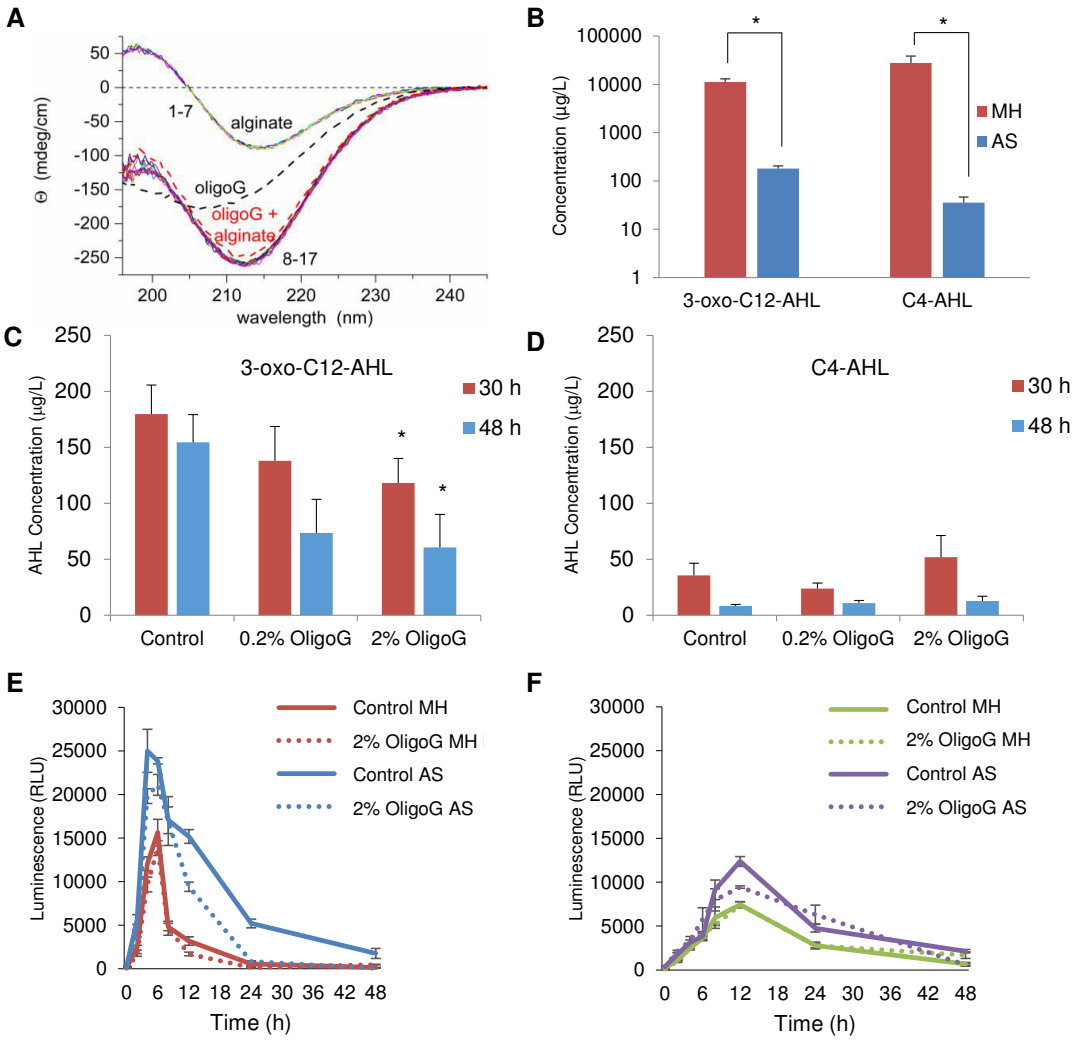

FIG 4 Effect of OligoG CF-5/20 on high Mw alginate and on cell signaling molecules *in vitro*. (A) Circular dichroism (CD) spectra of high Mw pseudomonal alginate mixed with OligoG CF-5/20. Scans 1-7 show spectra of high Mw alginate (~20 µM) followed over ~77 min upon heating from 4 to 37^{0}C; scans 8-11 (~44min) are recorded after addition of OligoG CF-5/20 (850 µM) followed by addition of Ca^{2+} (1mM) (scans 12-17, ~ 66min). Spectra of OligoG CF-5/20 (850 µM) alone and its sum with high Mw alginate (20 µM) are shown as black and red dashed lines, respectively. High performance liquid chromatography (HPLC) mass spectrometry (LC-QQQ-MS) to quantify acyl homoserine lactone (AHL; 3-oxo-C12-AHL and C4-AHL) production of *P. aeruginosa* PAO1 (B) grown in MH and AS medium (30 h), and in a time course assay (30 and 48 h) showing the effect of OligoG CF-5/20 on (C) 3-oxo C12-AHL and (D) C4-AHL (*$p<0.05$; n=3). Cell viability (ATP production) over 48 h of (E) PAO1 and (F) NH57388A grown in MH and AS medium ± 2% OligoG CF-5/20 (2%G).

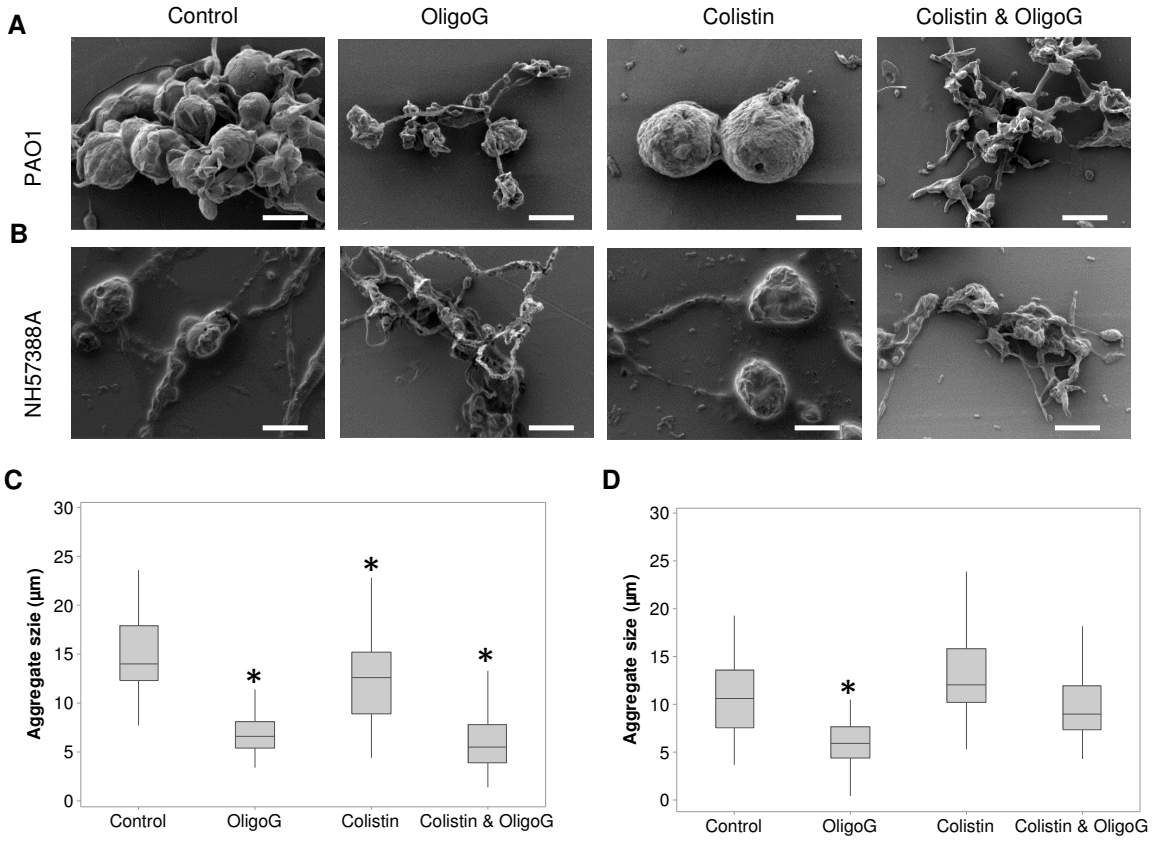

FIG 5 Biofilm disruption assays showing scanning electron microscopy (SEM) of antimicrobial (OligoG CF 5/20 and colistin) treated biofilms grown in ASM [Scale bar 10 µm]. SEM images of established (24 h) *P. aeruginosa* (A) PAO1 and (B) NH57388A biofilms treated for 24 h with 2% OligoG CF-5/20 ± colistin (16 µg/ml) with corresponding median microcolony diameter measurements for (C) PAO1 and (D) NH57388A (*p<0.05).